Linearized Integral Theory of Three-Dimensional Unsteady Flow in a Shear Layer

JOHN E. YATES*
Aeronautical Research Associates of Princeton, Inc., Princeton, N.J.

A linearized integral theory is developed for calculating the pressure on a perturbed wall in three-dimensional unsteady supersonic flow in the presence of a shear layer. An explicit formula for the wall pressure is given for an array of panels undergoing simple harmonic motion. Asymptotic and numerical results are presented for the kernel of the wall pressure. The integral theory reduces to the exact linearized inviscid theory in the limit of zero shear layer thickness. Also, it reduces to the two-dimensional steady-state theory of Ref. 1. For a finite layer, there are three integral thickness parameters. A critical Mach number is calculated (≈ 1.8) below which there is upstream influence and the kernel is attenuated by the shear layer. For supercritical Mach numbers, there is no upstream influence.

Nomenclature

b	= reference length
$f(x, y, t)$	= surface deflection function
$F(x, y)$	= amplitude of unsteady surface deflection
$g(y)$	= spanwise mode shape
Im	= imaginary part of complex quantity
$J(s)$	= $e^{i\Omega s}K_1(s)$, see Eqs. (49) and (50)
$J_o(z)$	= Bessel function, first kind order zero
k	= $\omega b/u_\infty$, reduced frequency
K	= $kM_\infty/\beta_\infty{}^2$
$L(\lambda, s)$	= special function, see Eq. (52)
M	= Mach number, see Eq. (4)
N	= index in power law velocity profile
P	= perturbation pressure, see Eq. (3)
$P_w{}^o$	= inviscid surface pressure, see Eq. (21)
Re	= real part of complex quantity
s	= Γx
t	= dimensionless time
u, v, w	= perturbation velocity components
$U(z)$	= mean velocity profile
x, y, z	= Cartesian coordinates, see Fig. 1
β_∞	= $(M_\infty{}^2 - 1)^{1/2}$
δ	= boundary-layer thickness
δ^*	= displacement thickness
$\delta_s, \delta_c, \delta_k, \delta_{ks}$	= basic integral thickness parameters, see Eqs. (24) and (56)
ε	= δ^*/b
θ	= mean temperature profile
$K(x, y)$	= kernel function, see Eq. (19)
$K_1(x)$	= reduced one-dimensional kernel
Π_w, ϕ_w	= wavy wall pressure amplitude and phase angle, see Eq. (59)
χ	= similarity parameter, see Eq. (60)
Ω	= KM_∞/Γ

Subscripts and Superscripts

	= total derivative
∞	= freestream condition
w	= wall condition
e	= condition at edge of boundary layer
$(\bar{\ })$	= Fourier transform, see Eq. (8)
o	= inviscid quantity

1. Introduction

THE problem of calculating aerodynamic forces on stationary or oscillating surfaces historically has been treated by inviscid aerodynamic theory. When the boundary-layer thickness is small compared to the characteristic length scale of the problem, one can argue that viscous effects caused by the boundary layer are indeed negligible. In particular, in the early work on the problem of panel flutter, inviscid aerodynamics theory was the primary tool.

When the Mach number is low supersonic and the boundary layer is not "too thin," it has been demonstrated by Muhlstein, Gaspers and Riddle[2] that the boundary layer has a significant effect on panel flutter. Further work by Muhlstein and Beranek[3] showed that the pressure amplitude and phase on a stationary wavy wall are strongly dependent on the boundary-layer thickness in the low supersonic regime.

Various theoretical efforts have been attempted to include the boundary layer in the usual inviscid aerodynamic theory. Some of the earlier approaches to the problem are contained in the work of Lighthill,[4] Benjamin,[5] Miles,[6] McClure,[7] Anderson and Fung,[8] and Zeydel.[9] More recently the problem has been attacked with a greater level of numerical success by Dowell and Ventres.[10] Their approach is to solve the inviscid perturbation equations in the shear flow along with the panel flutter problem. Ventres[11] has also developed a perturbation expansion (in terms of boundary-layer thickness) of Dowell's earlier theory. He has shown by comparison with experimental results that a direct perturbation expansion is only good for very thin boundary layers.

The approach taken in the present paper is to start from the basic perturbation equations in a shear flow and develop the asymptotic solution in terms of thickness by integral methods. The asymptotic solution agrees very well with experimental results on a wavy wall for boundary-layer thicknesses as large as one-half the disturbance wavelength.

2. Formulation of the Problem

We consider the supersonic flow over a wall that departs slightly from the x-y plane as shown in Fig. 1. The mean

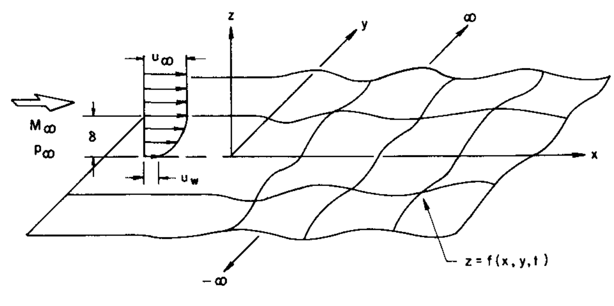

Fig. 1 Coordinate system and basic geometry.

Received June 14, 1973; revision received November 8, 1973. This work was sponsored by AFOSR Contract F44620-71-C-0132.
Index categories: Nonsteady Aerodynamics; Aeroelasticity and Hydroelasticity.

* Consultant.

flow is in the positive x direction. The mean turbulent boundary layer is modeled as a uniform shear layer of thickness delta. We assume at the outset of our analysis that viscosity does not directly affect the perturbation flowfield and furthermore that the viscous sublayer can be neglected. The mean velocity tends to a finite value at the wall.

The perturbation flowfield can thus be derived from the Euler equations and state equations. After elimination of the perturbation temperature, the equations for the perturbation pressure and velocity can be expressed in the dimensionless form

$$
\begin{aligned}
M_\infty{}^2 \frac{DP}{Dt} + \frac{\partial u}{\partial x} + \frac{\partial v}{\partial y} + \frac{\partial w}{\partial z} &= 0 \\
\frac{Du}{Dt} + U'w + \theta \frac{\partial P}{\partial x} &= 0 \\
\frac{Dv}{Dt} \qquad + \theta \frac{\partial P}{\partial y} &= 0 \\
\frac{Dw}{Dt} \qquad + \theta \frac{\partial P}{\partial z} &= 0
\end{aligned}
\tag{1}
$$

where

$$D/Dt = \partial/\partial t + U\,\partial/\partial x \tag{2}$$

and

$$P = \frac{p - p_\infty}{\rho_\infty u_\infty{}^2} = \frac{1}{\gamma M_\infty{}^2}\left(\frac{p}{p_\infty} - 1\right) \tag{3}$$

Also, $U(z)$ and $\theta(z)$ are, respectively, the dimensionless mean velocity and temperature profiles which become unity in the freestream. The local Mach number M is defined by the relation

$$M^2 = M_\infty{}^2 U^2/\theta \tag{4}$$

and the dimensional reference length and time are, respectively, b and b/u_∞. The boundary conditions on the perturbation flow are

$$w(x, y, 0, t) = \partial f/\partial t + U_w \partial f/\partial x \tag{5}$$

where

$$z = f(x, y, t) \tag{6}$$

is the perturbed wall shape and U_w is the mean velocity at the wall. In the freestream we require outgoing downstream propagating waves.

Next we introduce a simple harmonic wall disturbance

$$f = Re[F(x, y)e^{ikt}] \tag{7}$$

where $k = \omega b/u_\infty$ is the reduced frequency. Also, we introduce the double Fourier transform pair

$$
\begin{aligned}
\bar{q}(\xi, \eta) &= \iint_{-\infty}^{\infty} e^{-i(x\xi + y\eta)} q(x, y)\,dx\,dy \\
q(x, y) &= \frac{1}{(2\pi)^2} \iint_{-\infty}^{\infty} e^{i(x\xi + y\eta)} \bar{q}(\xi, \eta)\,d\xi\,d\eta
\end{aligned}
\tag{8}
$$

Substitute Eq. (7) into Eqs. (1) and (5) and take the double Fourier transform. After eliminating the u, v velocity components, we obtain the following pair of equations and boundary condition:

$$
\begin{aligned}
\frac{d\bar{W}}{dz} + \left[M_\infty{}^2 - \theta\frac{(\xi^2 + \eta^2)}{(U\xi + k)^2}\right]\bar{P} &= 0 \\
\frac{d\bar{P}}{dz} - \frac{(U\xi + k)^2}{\theta}\bar{W} &= 0 \\
\bar{W}(0) &= \bar{F}
\end{aligned}
\tag{9}
$$

where

$$\bar{W} = -i\bar{w}/(U\xi + k) \tag{10}$$

In the freestream, the coefficients in Eq. (9) are constant and the solution corresponding to outgoing waves gives us a simple relation between P and W; namely

$$\bar{P}_e = -\frac{(\xi + k)^2 \bar{W}_e}{\beta_\infty[K^2 + \eta^2/\beta_\infty{}^2 - (\xi + KM_\infty)^2]^{1/2}} \tag{11}$$

where the subscript e denotes a condition at the outer edge of the shear layer.

3. Integral Solution for the Wall Pressure

We solve Eqs. (9) and (11) in the limit that the shear layer thickness δ is small compared to the characteristic length of the wall disturbance. To lowest order we obtain the exact inviscid result

$$
\begin{aligned}
\bar{W} &= \bar{W}_w = \bar{F} \\
\bar{P} &= \bar{P}_w = -(\xi + k)^2 \bar{F}/\beta_\infty h^{1/2}(\xi, \eta)
\end{aligned}
\tag{12}
$$

where

$$
\begin{aligned}
h(\xi, \eta) &= K^2 + \eta^2/\beta_\infty{}^2 - (\xi + KM_\infty)^2 \\
K &= kM_\infty/\beta_\infty{}^2
\end{aligned}
\tag{13}
$$

To obtain the second-order result we integrate Eqs. (9) across the shear layer and use the boundary conditions at the wall and in the freestream

$$
\begin{aligned}
\bar{W}_e &= \bar{F} - \int_o^\delta \left[M_\infty{}^2 - \theta\frac{(\xi^2 + \eta^2)}{(U\xi + k)^2}\right]\bar{P}\,dz \\
\bar{P}_e &= \bar{P}_w + \int_o^\delta \frac{(U\xi + k)^2}{\theta}\bar{W}\,dz
\end{aligned}
\tag{14}
$$

Now substitute the lowest order results for $\bar{P}$ and $\bar{W}$ into the integral terms of Eq. (14) and solve for the wall pressure. We get

$$\bar{P}_w = -\frac{(\xi + k)^2 \bar{F}}{\beta_\infty h^{1/2}}\left[1 - \frac{f(\xi, \eta)}{h^{1/2}} + O(\delta^2)\right] \tag{15}$$

or to the same order of validity in δ

$$\bar{P}_w = -\frac{(\xi + k)^2 \bar{F}}{\beta_\infty[h^{1/2}(\xi, \eta) + f(\xi, \eta)]} + O(\delta^2) \tag{16}$$

where

$$
\begin{aligned}
f(\xi, \eta) = -\frac{1}{\beta_\infty}\int_o^\delta \Bigg\{&\frac{\beta_\infty{}^2}{\theta}\left(\frac{U\xi + k}{\xi + k}\right)^2 h(\xi, \eta) - \\
&\theta\left(\frac{\xi + k}{U\xi + k}\right)^2\left[\xi^2 + \eta^2 - M_\infty{}^2\frac{(U\xi + k)^2}{\theta}\right]\Bigg\}dz
\end{aligned}
\tag{17}
$$

The simple step of inverting the perturbation term in Eq. (15) is a crucial one from the standpoint of practical calculations. The direct perturbation expansion, Eq. (15), leads to divergent results for disappointingly small boundary-layer thicknesses.[11] We shall see below that the inverted form, Eq. (16), yields uniform self-consistent results even for $\delta = 0(1)$.

Now take the inverse Fourier transform of Eq. (16) to obtain the formal expression for the wall pressure

$$P_w(x, y) = \frac{1}{\beta_\infty}\iint_{-\infty}^{\infty} \mathrm{K}(x - \xi, y - \eta)\left(\frac{\partial}{\partial \xi} + ik\right)^2 F(\xi, \eta)\,d\xi\,d\eta \tag{18}$$

where the kernel function

$$\mathrm{K}(x, y) = \frac{1}{(2\pi)^2}\iint_{-\infty}^{\infty} \frac{e^{i(x\xi + y\eta)}}{h^{1/2}(\xi, \eta) + f(\xi, \eta)}\,d\xi\,d\eta \tag{19}$$

The complete first-order effect of the shear layer is contained in the function $f(\xi, \eta)$ given by Eq. (17). In the complete absence of a shear layer, the kernel can easily be evaluated in closed form. We have

$$
\begin{aligned}
\mathrm{K}_o(x, y) &= \frac{1}{(2\pi)^2}\iint_{-\infty}^{\infty} \frac{e^{i(x\xi + y\eta)}}{h^{1/2}(\xi, \eta)}\,d\xi\,d\eta \\
&= \frac{\beta_\infty}{\pi} e^{-iKM_\infty x} \frac{\cos K(x^2 - \beta_\infty{}^2 y^2)^{1/2}}{(x^2 - \beta_\infty{}^2 y^2)^{1/2}} \qquad x > \beta_\infty |y| \\
&= 0 \qquad x < \beta_\infty |y|
\end{aligned}
\tag{20}
$$

and

$$
\begin{aligned}
P_w{}^o(x, y) = \frac{1}{\pi}\int_{-\infty}^{x} d\xi \int_{y - (x - \xi)/\beta_\infty}^{y + (x - \xi)/\beta_\infty} d\eta\, e^{-iKM_\infty(x - \xi)} \times \\
\frac{\cos K[(x - \xi)^2 - \beta_\infty{}^2(y - \eta)^2]^{1/2}}{[(x - \xi)^2 - \beta_\infty{}^2(y - \eta)^2]^{1/2}}\left(\frac{\partial}{\partial \xi} + ik\right)^2 F(\xi, \eta)
\end{aligned}
\tag{21}
$$

which is the exact inviscid expression for the wall pressure.[12] The integration is over the upstream facing Mach cone.

The evaluation of the kernel for any finite boundary-layer thickness is a formidable task if we anticipate the use of the integral definition of $f(\xi,\eta)$ given by Eq. (17). However, a remarkable simplification is obtained if we expand the integral expression for

$$k < U_w|\xi| \tag{22}$$

To first-order in k we obtain a biquadratic expression for f; namely

$$f(\xi,\eta) \cong \delta_s\xi^2 - 2k\delta_k\xi + \delta_c\eta^2 \tag{23}$$

where

$$\begin{aligned}
\delta_s &= \frac{1}{\beta_\infty}\int_o^\delta\left(1-\frac{M^2}{M_\infty^{\ 2}}\right)\left(\frac{M_\infty^{\ 2}}{M^2}-\beta_\infty^{\ 2}\right)dz\\
\delta_c &= \frac{1}{\beta_\infty}\int_o^\delta\left(\frac{M_\infty^{\ 2}}{M^2}-\frac{M^2}{M_\infty^{\ 2}}\right)dz\\
\delta_k &= \frac{1}{\beta_\infty}\int_o^\delta\left[M_\infty^{\ 2}-M^2+\left(\frac{1}{U}-1\right)\left(\frac{M_\infty^{\ 2}}{M^2}+\frac{M^2}{M_\infty^{\ 2}}-M^2\right)\right]dz
\end{aligned} \tag{24}$$

Physically, the restriction imposed by Eq. (22) is that the wave speed of the surface disturbance must be less than the surface mean velocity U_w which is the velocity at the edge of the viscous sublayer. For consistency, this condition must be met in application of the results. We emphasize that the frequency limitation is only imposed on the boundary-layer contribution to the kernel. Exact inviscid frequency effects are retained throughout the following discussion.

The parameters δ_s, δ_c, δ_k in Eq. (24) are fundamental to the integral perturbation theory. Each parameter is a function of the freestream Mach number and the particular mean velocity and temperature profile chosen. The ratio of each parameter to the displacement thickness is plotted vs M_∞ in Fig. 2 for a $\frac{1}{7}$th power law velocity profile and adiabatic wall with unit Prandtl number. The ratio δ_s/δ^* is the two-dimensional steady-state effect of the boundary layer. It is positive for $M_\infty < M_c$ and negative for $M_\infty > M_c$. The "critical" Mach number M_c is approximately 1.79 for the $\frac{1}{7}$th profile. The sign change in δ_s has the important consequence that the boundary layer only has upstream influence for $M_\infty < M_c$ (see Sec. 6). The three-dimensional effect of the boundary layer is contained in the parameter δ_c which decays with increasing Mach number. The parameter δ_k is the first-order unsteady boundary-layer effect and has a minimum around $M_\infty = 2$. Each parameter becomes quite large near $M_\infty = 1$, where we expect the largest boundary-layer effect on the inviscid result.

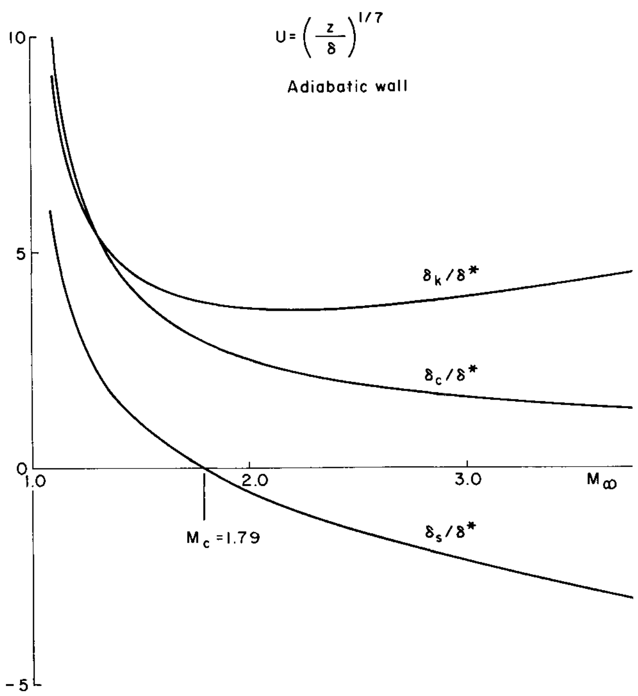

Fig. 2 Integral thicknesses vs Mach number.

Finally, we remark that we have tacitly assumed $U_w = 0$ in the evaluation of the integral parameters. The maximum error incurred is in the parameter δ_k which has the strongest singularity in the integrand. For a power law profile with index N, the error is readily estimated to be

$$\varepsilon_k = \frac{1}{\beta_\infty}\left(1+\frac{\gamma-1}{2}M_\infty^{\ 2}\right)\frac{U_w^{\ N-3}}{(1-3/N)\delta_k} \tag{25}$$

A typical calculation at $M_\infty = 1.1$ with $N = 7$ and $\gamma = 1.4$ shows that the error is less than 4% if $U_w < \frac{1}{3}$. The error is even less at moderate values of the Mach number.

4. Evaluation of the Kernel

Even with the foregoing simplification, evaluation of the kernel for an arbitrary wall is not a simple task. Here we consider two special cases: 1) wall deflection independent of y, and 2) wall deflection simple harmonic in y.

When the wall deflection and pressure are independent of y, we derive a single integral expression for the wall pressure. From Eqs. (18) and (19) we get

$$P_w(x) = \frac{1}{\beta_\infty}\int_{-\infty}^{\infty} K_1(x-\xi)\left(\frac{\partial}{\partial\xi}+ik\right)^2 F(\xi)\,d\xi \tag{26}$$

where

$$K_1(x) \equiv \int_{-\infty}^{\infty} K(x,y)\,dz = \frac{1}{2\pi}\int_{-\infty}^{\infty}\frac{e^{ix\xi}}{h^{1/2}(\xi,0)+f(\xi,0)}d\xi \tag{27}$$

The reduced or one-dimensional kernel can be simplified further for steady-state deflections. We get

$$K_1(x) = \frac{1}{2\pi i}\int_{-\infty}^{\infty}\frac{e^{ix\xi}}{\xi}d\xi - \frac{1}{2\pi i}\int_{-\infty}^{\infty}\frac{e^{ix\xi}}{\xi+i/\delta_s}d\xi,\ k=0 \tag{28}$$

There are two cases that depend upon the sign of δ_s:

Subcritical $M_\infty < M_c$ and $\delta_s > 0$

$$\begin{aligned} K_1(x) &= e^{x/\delta_s} \qquad x<0\\ &= 1 \qquad\quad\ \ x>0 \end{aligned} \tag{29}$$

Supercritical $M_\infty > M_c$ and $\delta_s < 0$

$$\begin{aligned} K_1(x) &= 0 \qquad\qquad x<0\\ &= 1-e^{x/\delta_s} \quad x>0 \end{aligned} \tag{30}$$

For the one-dimensional steady-state case, the kernel depends upon the single integral parameter δ_s. The importance of δ_s in determining the presence of upstream influence is evident from these simple results.

When the wall deflection has a simple harmonic dependence on y, we proceed as follows: Let

$$F(x,y) = F(x)\sin\pi y \qquad -\infty < y < \infty \tag{31}$$

Substitute Eq. (31) into Eq. (18) and carry out the η integration using Eq. (19). We get

$$P_w(x,y) = P_w(x)\sin\pi y \tag{32}$$

where

$$P_w(x) = \frac{1}{\beta_\infty}\int_{-\infty}^{\infty} K_1(x-\xi)\left(\frac{\partial}{\partial\xi}+ik\right)^2 F(\xi)\,d\xi \tag{33}$$

and

$$K_1(x) = \frac{1}{2\pi}\int_{-\infty}^{\infty}\frac{e^{ix\xi}}{h^{1/2}(\xi,\pi)+f(\xi,\pi)}d\xi \tag{34}$$

We observe that the kernel Eq. (34) differs from Eq. (27) only in the constant value of η in the denominator of the integrand. More generally an arbitrary periodic spanwise deflection can be treated where the constant argument for η becomes

$$\eta = (c)^{1/2} = \left(\int_o^1 g'^2\,dy\right)^{1/2} \tag{35}$$

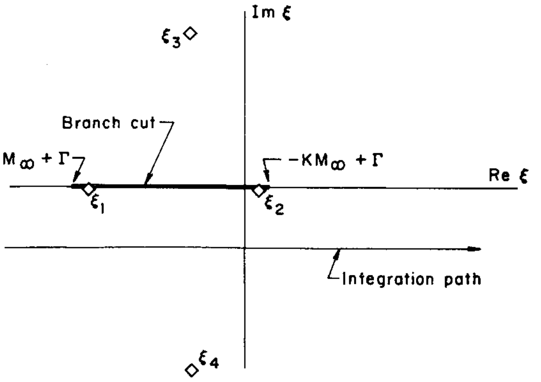

Fig. 3 Inverse Fourier transform plane.

where $g(y)$ is the assumed deflection over a single period. This operation is equivalent to carrying out a single mode Galerkin analysis in the spanwise direction (for further detail, see Ref. 13).

The reduced one-dimensional kernel Eq. (34), or more generally

$$K_1(x) = \frac{1}{2\pi}\int_{-\infty}^{\infty} \frac{e^{ix\xi}}{h^{1/2}[\xi,(c)^{1/2}]+f[\xi,(c)^{1/2}]}d\xi \tag{36}$$

can be evaluated completely in terms of known functions. Denote the inverse transform by $\mathscr{F}^{-1}$ so that

$$\begin{aligned} K_1(x) &= \mathscr{F}^{-1}\frac{h}{h-f^2}\cdot\frac{1}{h^{1/2}} - \mathscr{F}^{-1}\frac{f}{h-f^2} \\ &= \int_o^\infty K_o(\xi)D(x-\xi)\,d\xi - G(x) \end{aligned} \tag{37}$$

where

$$\begin{aligned} D(x) &= \frac{1}{2\pi}\int_{-\infty}^{\infty} e^{ix\xi}\frac{h}{h-f^2}d\xi \\ G(x) &= \frac{1}{2\pi}\int_{-\infty}^{\infty} e^{ix\xi}\frac{f}{h-f^2}d\xi \end{aligned} \tag{38}$$

and

$$\begin{aligned} K_o(x) &= 0 & x<0 \\ &= e^{-iKM_\infty x}J_o(\Gamma x) & x>0 \end{aligned} \tag{39}$$

with

$$\Gamma = (K^2 + c/\beta_\infty{}^2)^{1/2} \tag{40}$$

The function $K_o(x)$ is the exact inviscid kernel. Furthermore, in the limit as δ and hence f tend to zero, we have

$$\begin{aligned} D(x) &\sim \delta(x) \quad \text{Dirac Delta Function} \\ G(x) &\sim 0 \end{aligned} \tag{41}$$

so that

$$K_1(x) \sim K_o(x) \qquad \text{as} \qquad \delta \to 0 \tag{42}$$

and we recover the exact inviscid result in the limit.

For a finite boundary-layer thickness, the denominator of the integrals in Eq. (38) is a fourth degree polynomial

$$P(\xi) = h(\xi) - f^2(\xi) \tag{43}$$

with roots ξ_n, $n = 1, 2, 3, 4$. These roots are located in the complex ξ plane as shown in Fig. 3. The branch points of $h^{1/2}(\xi)$ are located at $-KM_\infty \pm \Gamma$ as shown and the roots $\xi_{1,2}$ are located near the branch points on the real axis but under the branch cut. The path of integration for the inverse transform must lie above the root ξ_4 and below the real axis to obtain a kernel that is finite for all x.

Now define the coefficients

$$A_n = if(\xi_n)/P'(\xi_n), \qquad B_n = ih(\xi_n)/P'(\xi_n) \tag{44}$$

and note that

$$\frac{1}{P(\xi)} = \sum_{n=1}^{4}\frac{1}{P'(\xi_n)(\xi-\xi_n)} \tag{45}$$

Then $D(x)$ and $G(x)$ can be evaluated explicitly in terms of exponentials

$$\begin{aligned} D(x) &= -B_4 e^{ix\xi_4}, & x<0 \\ &= \sum_{n=1}^{3} B_n e^{ix\xi_n}, & x>0 \\ G(x) &= -A_4 e^{ix\xi_4}, & x<0 \\ &= \sum_{n=1}^{3} A_n e^{ix\xi_n}, & x>0 \end{aligned} \tag{46}$$

Because of the fact that δ_s changes sign at the critical Mach number, we have the following relations between A_n and B_n:

$$\begin{aligned} B_n/h^{1/2}(\xi_n) &= A_n, & n = 1,2 \\ &= -A_n(-1)^n \operatorname{sign}\delta_s, & n = 3,4 \end{aligned} \tag{47}$$

Also, it is easily shown by contour integration that

$$\begin{aligned} \sum_{n=1}^{4} A_n &= 0 \\ \sum_{n=1}^{n} \xi_n A_n &= -i/\delta_s \end{aligned} \tag{48}$$

When the foregoing results are substituted into Eq. (37), we obtain the following explicit representation of the kernel:

Subcritical $M_\infty < M_c$ and $\delta_s > 0$

$$\begin{aligned} J(s) \equiv e^{i\Omega s}K_1(s) &= 2A_4 e^{\lambda_4 s}, & s<0 \\ &= -\Gamma^{-1}\sum_{n=1}^{4} B_n L(\lambda_n, s), & s>0 \end{aligned} \tag{49}$$

Supercritical $M_\infty > M_c$ and $\delta_s < 0$

$$\begin{aligned} J(s) \equiv e^{i\Omega s}K_1(s) &= 0 & s<0 \\ &= -2A_3 e^{\lambda_3 s} - \Gamma^{-1}\sum_{n=1}^{4} B_n L(\lambda_n, s), & s>0 \end{aligned} \tag{50}$$

where

$$\begin{aligned} s = \Gamma x, &\qquad \Omega = KM_\infty/\Gamma \\ \lambda_n = i(\xi_n + KM_\infty)/\Gamma, &\qquad n = 1, 2, 3, 4 \end{aligned} \tag{51}$$

and

$$L(\lambda, s) = e^{\lambda s}\int_s^\infty e^{-\lambda t}J_o(t)\,dt, \qquad Re\lambda > 0 \tag{52}$$

The function $L(\lambda, s)$ is defined in the left half of the complex λ-plane by analytic continuation with a cut between the branch points at $\lambda = \pm i$. It is bounded for all λ's distinct from the branch points and in particular

$$|L(\lambda, s)| \sim 0[1/(s)^{1/2}], \qquad s \sim \infty, \quad \lambda \neq \pm i \tag{53}$$

A detailed algorithm for calculating L is given in the Appendix of Ref. 13.

5. Analytic Properties of the Kernel

Physically, the kernel is the pressure produced downstream of a line disturbance in the curvature and/or acceleration of the wall [see Eq. (26)]. Many properties of the kernel can be deduced analytically. We discuss a few of these below.

Continuity

The kernel is a continuous function of x for all x. To prove continuity we only need to consider the points at infinity and the origin. From the bounded property of L we deduce at once that

$$|J(s)| = |K_1(s)| \sim 0[1/(s)^{1/2}] \quad \text{for} \quad s \to \infty \tag{54}$$

Upstream, the supercritical kernel is identically zero, while subcritical it decays exponentially on a length scale of $0(\delta_s)$. The important property of upstream influence in subcritical flow is determined solely by the sign of δ_s even in the three-dimensional unsteady case.

At the origin we have

$$\lim_{s\to o^-} \mathrm{K}_1(s) - \lim_{s\to o^+} \mathrm{K}_1(s) = \sum_{n=1}^{4} A_n = 0 \tag{55}$$

so that K_1 is continuous at $s = 0$.

Asymptotic Behavior for Small δ

In the limit as $\delta \to 0$ we derive a concise approximation of the parameters that enter into the kernel. Omitting the details, we obtain the following results by straightforward asymptotic analysis:

$$\begin{aligned}
A_{1,2} &= \pm i f(z_{1,2})/2\Gamma + 0(\delta^3) \\
A_{3,4} &= \frac{\mp \operatorname{sign} \delta_s}{2(1 \mp 2ik\delta_{ks} \operatorname{sign} \delta_s)} + 0(\delta^2) \\
B_{1,2} &= \pm i f^2(z_{1,2})/2\Gamma + 0(\delta^4) \\
B_{3,4} &= \pm 1/2|\delta_s| + 0(\delta) \\
\lambda_{1,2} &= \mp i \pm f^2(z_{1,2})/2\Gamma^2 + 0(\delta^4) \\
\lambda_{3,4} &= \mp 1/\Gamma\,|\delta_s| + 2ik\delta_{ks}/\delta_s + 0(\delta) \\
z_{1,2} &= -KM_\infty \mp \Gamma \\
\delta_{ks} &= \delta_k + M_\infty{}^2\delta_s/\beta_\infty{}^2
\end{aligned} \tag{56}$$

where the upper sign belongs to first index in each expression. For sufficiently small δ these expressions can be used to evaluate $\mathrm{K}_1(s)$ numerically with Eqs. (49) and (50) (see Sec. 6).

When s is very large and δ is small the dominant terms in the summation over B_n in Eqs. (49) and (50) are for $n = 3, 4$. Furthermore, it is easily proved by integration by parts in Eq. (52) that for any s

$$L(\lambda, s) = J_o(s)/\lambda + 0(1/|\lambda|^2), \qquad |\lambda| \sim \infty \tag{57}$$

Thus, we can write for large s and small δ

$$J(s) \sim J_o(s) \qquad \text{for} \qquad s \to \infty \tag{58}$$

When $\delta \to 0$ for fixed s we recover the inviscid result in sub- and supercritical flow.

6. Numerical Examples of the Kernel

The simplest possible kernel is the two-dimensional steady-state result [see Eqs. (29) and (30)]. This kernel is a function of $x/|\delta_s|$ and the most important property to note is the upstream influence for $M_\infty < M_c$ and absence of the same for $M_\infty > M_c$. The pressure on a two-dimensional wavy wall corresponding to this simple kernel was developed in detail in Ref. 1 and compared with the experimental work of Muhlstein and Beranek.[2] We reproduce in Fig. 4 the key summary plot of Ref. 1. The pressure phase angle ϕ_w and amplitude Π_w are related to the parameter χ by the following relations [see Eqs. (3.20) and (3.21) of Ref. 1]:

$$\begin{aligned}
M_\infty < 1:\quad & \Pi_w = 1/(1+\chi) \sim 1 - \chi \\
& \phi_w = \pi \\
M_\infty > 1:\quad & \Pi_w = 1/(1+\chi^2)^{1/2} \sim 1 - \chi^2/2 \\
& \phi_w = \pi/2 + \tan^{-1}\chi \sim \pi/2 + \chi
\end{aligned} \tag{59}$$

where

$$\chi = (2\pi/\lambda)\cdot(\beta_\infty/|\beta_\infty|)\cdot\delta_s \tag{60}$$

and λ is the wavelength of the wall disturbance. The agreement between the theory and experiments is remarkable even for relatively large values of χ. On the other hand, the direct perturbation expansion of the amplitude in powers of χ (dashed curve in Fig. 4) tends to break down for somewhat smaller values of χ. However, the comparison is not as bad as results of Ventres[11] would indicate; in particular, the linear variation of the phase angle.

The significance of χ (or δ_s) as a basic viscous similarity parameter in the low supersonic regime is also evident from Fig. 4. Further details of the two-dimensional steady theory are given in Ref. 1.

The complete three-dimensional unsteady kernel was evaluated numerically with the asymptotic formula given by Eqs. (56) substituted into Eqs. (49) and (50). Because of slight numerical differences in the asymptotic approximations for positive and negative s, we have omitted the vicinity of the origin in the subsequent plots of the kernel. The kernels are calculated for a $\frac{1}{7}$th power law profile and adiabatic wall with Prandtl number unity. The integral parameters are given in Fig. 2.

In Fig. 5, the three-dimensional steady-state kernel at $M_\infty = 1.35$ and 2.0 is plotted for several values of the displacement thickness parameter $\varepsilon = \delta^*/b$. It is a real function for $k = 0$. For the subcritical Mach number 1.35, we note the upstream influence and the attenuating effect of the boundary layer downstream of the source. Supercritical, $M_\infty = 2$, the significant feature is the absence of upstream influence.

In Fig. 6, the full kernel K_1 and the function $J(s)$ which has the inviscid complex phase factor $e^{i\Omega s}$ removed [see Eqs. (49) and (50)] are plotted for $M_\infty = 1.1$ and boundary-layer thickness

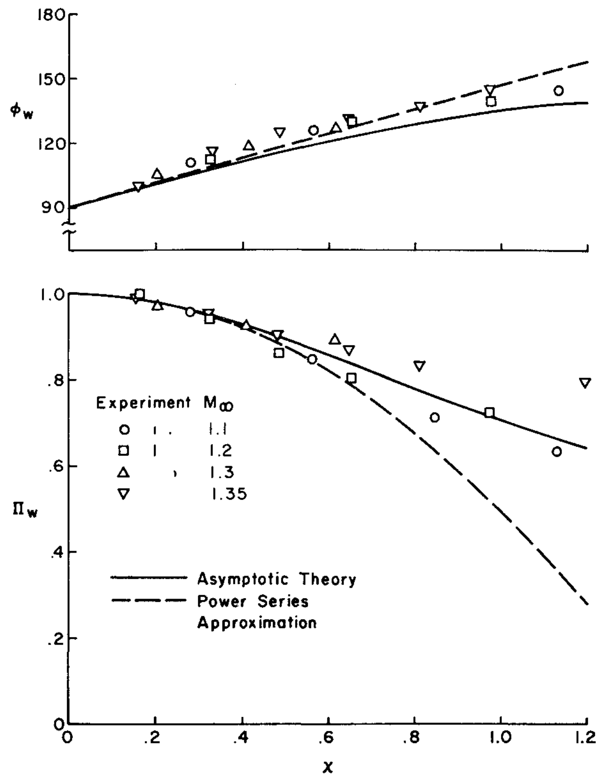

Fig. 4 Wall pressure amplitude and phase angle vs similarity parameter χ for a $\frac{1}{7}$th power law profile.

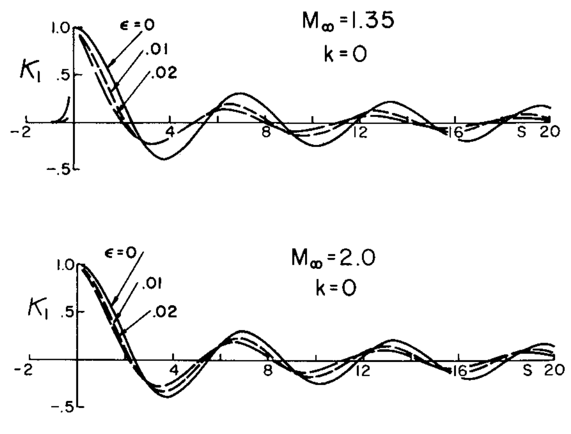

Fig. 5 Three-dimensional steady-state kernel.

$\varepsilon = 0.01$ for several values of the reduced frequency. We note that the real or in-phase part of $J(s)$ is insensitive to changes in reduced frequency. Also, for the low Mach number $M_\infty = 1.1$ the upstream influence is very pronounced and the real part is strongly damped at downstream points. The real part of K_1 is much more sensitive to reduced frequency than J, particularly at downstream points. The imaginary or out-of-phase part of J and K_1 has a smaller amplitude but is more dependent on reduced frequency.

Similar results are plotted in Fig. 7 at $M_\infty = 2.0$ and $\varepsilon = 0.02$. The absence of upstream influence is again noted. Also, we observe that even for relatively large values of k, the real part of J depends weakly on frequency. The predominant frequency effect is the inviscid phase factor. In conclusion, we remark that during this work, a typical kernel was computed for a $\frac{1}{7}$th and $\frac{1}{9}$th power law velocity profile. The difference in the results is negligibly small. This result is consistent with our basic assumption where we neglect the viscous sublayer and the direct effect of viscosity on the perturbation flowfield.

7. Conclusions

The linearized integral theory developed in Ref. 1 is extended to the case of three-dimensional unsteady disturbances. The principal result of the theory is an integral expression for the wall pressure [see Eq. (18)] that involves a kernel function $K_1(x)$. In the limit of no shear layer, K_1 reduces to the exact inviscid kernel. The total effect of the shear layer is contained in three integral thickness parameters δ_s, δ_k and δ_c that are, respectively, the effect of two-dimensional steady-state disturbances, unsteadiness, and three-dimensionality. The main conclusions of the study are the following:

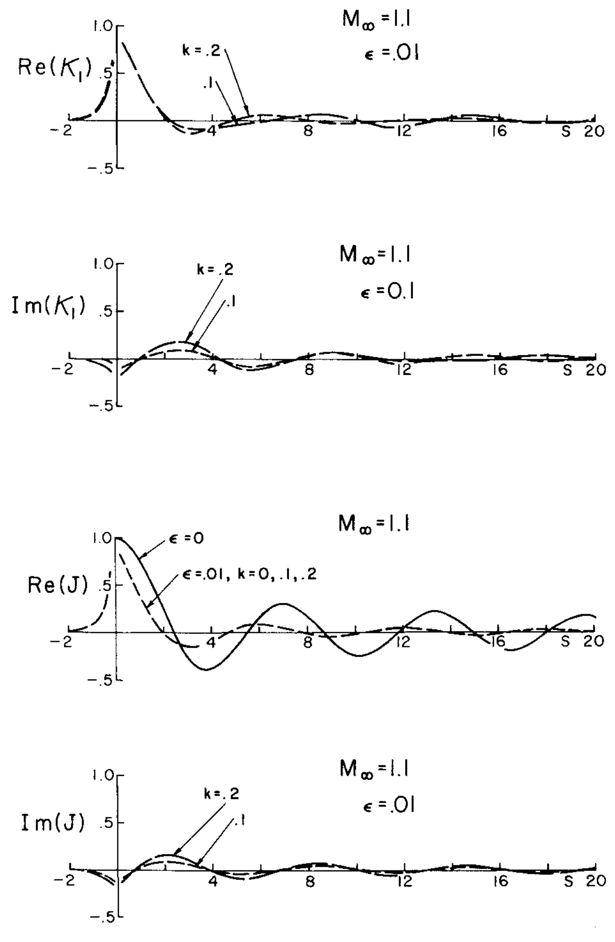

Fig. 6 Three-dimensional unsteady kernel at $M_\infty = 1.1$ and $\varepsilon = 0.01$.

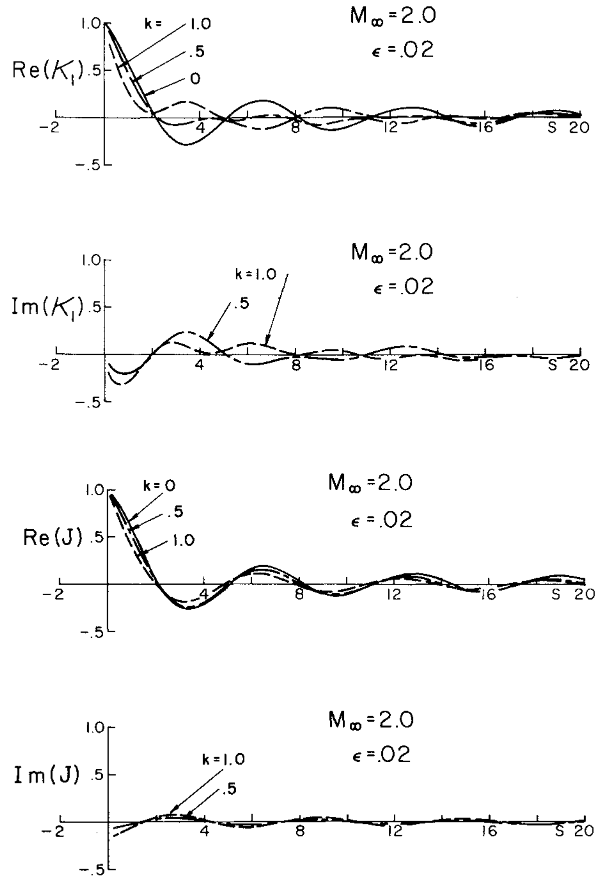

Fig. 7 Three-dimensional unsteady kernel at $M_\infty = 2.0$ and $\varepsilon = 0.02$.

1) The basic integral thickness parameters and the kernel are not sensitive to the precise turbulent velocity profile used.

2) The three-dimensional unsteady kernel contains upstream influence only for M_∞ less than the critical Mach number $M_c \approx 1.8$ where $\delta_s > 0$.

3) The boundary layer attenuates the inviscid kernel function at all downstream points for sub- and supercritical flow.

4) The subcritical kernel tends uniformly to the exact inviscid kernel for vanishing boundary-layer thickness. The supercritical kernel is uniform except in a layer of thickness δ_s near the origin where the amplitude grows rapidly to the inviscid value.

It is suggested that the theory developed herein be used to investigate panel flutter instability in the low supersonic regime. Furthermore, it is recommended that the transform method developed by Zeydel and Yates[13] be employed. The Fourier transform of the wall pressure [see Eq. (16)], including the shear layer, poses very little additional complexity over the inviscid pressure when the Fourier transform method is used.

It is further suggested that the theory be used to study the ablation problem and to investigate the lift on transonic airfoils or control surfaces where boundary-layer effects can be significant. In this regard, Dowell and Ventres[14] have recently shown the basic method for calculating the lifting surface kernel function with boundary layer effects included.

References

[1] Yates, J. E., "Linearized Integral Theory of the Viscous Compressible Flow Past a Wavy Wall," AFOSR-TR-72-1335, July 1972, Aeronautical Research Associates of Princeton, Princeton, N.J.

[2] Muhlstein, L., Jr., Gaspers, P. A., Jr., and Riddle, D. W., "An Experimental Study of the Influence of the Turbulent Boundary Layer on Panel Flutter," TN-D-4486, 1968, NASA; see also TN D-5798, May 1970, NASA.

[3] Muhlstein, L., Jr. and Beranek, R. G., "Experimental Investigation

of the Influence of the Turbulent Boundary Layer on the Pressure Distribution over a Rigid Two-Dimensional Wavy Wall," TN D-6477, Aug. 1971, NASA.

[4] Lighthill, M. J., "On Boundary Layers and Upstream Influence II. Supersonic Flows without Separation," *Proceedings of the Royal Society*, Vol. A217, 1953, pp. 478 and 504; see also *Quarterly Journal of Mechanics*, Vol. 3, 1950, p. 303.

[5] Benjamin, T. B., "Shearing Flow over a Wavy Boundary," *Journal of Fluid Mechanics*, Vol. 6, 1959, p. 161.

[6] Miles, J. W., "On Panel Flutter in the Presence of a Boundary Layer," *Journal of Aerospace Sciences*, Vol. 26, No. 2, Feb. 1959, pp. 81–93.

[7] McClure, J. D., "On Perturbed Boundary Layer Flows," Rept. 62-2, June 1962, M.I.T. Fluid Dynamic Research Lab., Cambridge, Mass.

[8] Anderson, W. J. and Fung, Y. C., "The Effect of an Idealized Boundary Layer on the Flutter of Cylindrical Shells in Supersonic Flow," GALCIT Structural Dynamics Rept. SM62-49, Dec. 1962, Graduate Aeronautical Lab., California Institute of Technology, Pasadena, Calif.

[9] Zeydel, E. F. E., "Study of the Pressure Distribution on Oscillating Panels in Low Supersonic Flow with Turbulent Boundary Layer," NASA CR-691, Feb. 1967, Georgia Institute of Technology, Atlanta, Ga.

[10] Dowell, E. H., "Generalized Aerodynamic Forces on a Flexible Plate Undergoing Transient Motion in a Shear Flow with an Application to Panel Flutter," *AIAA Journal*, Vol. 9, No. 5, May 1971, pp. 834–841.

[11] Ventres, C. S., "Transient Panel Motion in a Shear Flow," AMS Rept. 1062, Aug. 1972, Princeton Univ., Princeton, N.J.

[12] Garrick, I. E. and Rubinow, S. I., "Theoretical Study of Air Forces on an Oscillating or Steady Thin Wing in a Supersonic Main Stream," TN 1383, July 1947, NACA.

[13] Yates, J. E., "A Study of Panel Flutter with the Exact Method of Zeydel," NASA CR-1721, Dec. 1970, Aeronautical Research Associates of Princeton, Princeton, N.J.

[14] Dowell, E. H. and Ventres, C. S., "Derivation of Aerodynamic Kernel Functions," *AIAA Journal*, Vol. 11, No. 11, Nov. 1973, pp. 1586–1588.

MAY 1974 AIAA JOURNAL VOL. 12, NO. 5

Effect of the Adverse Pressure Gradient on Vortex Breakdown

TURGUT SARPKAYA*
Naval Postgraduate School, Monterey, Calif.

The present work examines in detail the effect of the degree of divergence on the type and location of the vortex breakdown in swirling flows in tubes of various angles of divergence, compares the results with those predicted through the use of the analytical models proposed by Randall and Leibovich and by Mager, and illustrates the role played by the flow separation and reversal on the tube wall.

Nomenclature

a = normalized core area ($= \delta^2$)
A = normalized tube area
b_{ij} = a variable coefficient
D_o = minimum tube diameter ($= 2r_o$)
f_{ij} = functions of α, β, and a/A
I_{ij} = massflow and momentum deficiency integrals
K_{ij} = a variable coefficient
L = length of the diverging tube
m = const
M = massflow coefficient ($=$ massflow$/\pi\rho r_o{}^2 V_o'$)
p = static pressure
P = total pressure
r, z = radial and axial coordinates
r_o = minimum radius of the tube
r_b = tube wall radius
R_i = radial distance to the tip of a vane
Re = Reynolds number
S = swirl coefficient ($= \Gamma/r_o W_o$)
u, v, w = flow velocities in cylindrical coordinates
V_i = uniform velocity between two vanes
W = value of w outside the vortex core
$W_o, \bar{W}_o$ = maximum velocity and mean velocity at $z = 0$
α = ratio of axial velocities ($= w_o/W$)
β = a parameter
γ = half angle of divergence
Γ = circulation
δ = core radius
η = normalized radial distance ($= r/\delta$)
θ = vane angle
ν = kinematic viscosity
ρ = density
Ω = normalized circulation ($= \Gamma/\bar{W}_o D_o$)
$(\ )'$ = differentiation with respect to z

Received August 14, 1973; revision received November 7, 1973. The author wishes to thank Lt. G. Treiber for his assistance with the experiments.

Index categories: Viscous Nonboundary-Layer Flows; Hydrodynamics.

* Professor of Mechanical Engineering. Member AIAA.

Introduction

THIS paper is the sequel to the author's two previous publications.[1,2] The first of these emphasized the existence of a range of breakdown patterns, from a double-helix sheet to a highly axisymmetric bubble, and examined the swirl-angle distribution, variation of the axial velocity, and the characteristics of traveling vortex breakdowns. The second described the additional observations made and discussed the results in the context of existing theories. Here attention is directed to the effect of the adverse pressure gradient on the position of occurrence and the form of the vortex breakdown.

Despite numerous analytical and experimental attempts, which are aptly summarized by Hall,[3] the explanation of the mechanism giving rise to the vortex breakdown has withstood attack and remains a source of controversy. Consequently, little progress has been made towards the prediction of the effect of the occurrence or use of the vortex breakdown on delta wings, in suction tubes of pumps, in draft tubes of turbines, in flame holders and combustion chambers, in trailing vortices behind wings, etc., just to name a few of a variety of practical circumstances in which the vortex breakdown has favorable or unfavorable effects.